World Applied Sciences Journal 38 (2): 91-100, 2020
ISSN 1818-4952
© IDOSI Publications, 2020
DOI: 10.5829/idosi.wasj.2020.91.100

Wavelet Steganographic Method for Colour Images

[1]B.E. Carvajal-Gámez, [2]F.J. Gallegos-Funes and [2]J. López-Bonilla

[1]SEPI-ESCOM, Instituto Politécnico Nacional, Av. Bátiz S/N, 07738, CDMX, México
[2]ESIME-Zacatenco, Instituto Politécnico Nacional, Col. Lindavista 07738, CDMX

Abstract: We exhibit a steganographic method for color images using variance field estimation and scaling factor for energy conservation.

Key words: Steganography · Scaling factor · Variance field estimation · Stegoanalysis · Discrete wavelet transform

INTRODUCTION

Steganography involves the secret data communications in an appropriate multimedia carrier (i.e. audio, image and video files), under the assumption that if the secret data is visible, the point of attack is evident [1, 3], thus the goal here is to conceal the existence of the embedded data. In the case of image files, a steganographic method employs innocent-looking media called host or cover image to imperceptibly carry hidden data to an intended recipient [1-3]. The image embedded with the hidden data (i.e. secret data, copyright notice, serial number) is called the stego-image and it looks as a normal image. The steganalysis techniques detect the existence of secret data in digital media, these techniques are designed to distinguish between the cover and stego-images [4, 5].

Steganographic techniques can be classified in spatial, frequency and adaptive methods [1]. The *spatial methods* generally use a technique to replace the direct least significant bit (LSB) substituting a redundant part of a cover image with a secret message. The *methods based in frequency domain*, such as the Fourier transform (FT), the discrete cosine transform (DCT) and the discrete wavelet transform (DWT) embed secret information in the frequency domain of a cover image. These methods hide messages in significant areas of the cover image which makes them more robust to attacks, such as compression, cropping and some image processing, than the LSB approach [1]. Recently there exist methods such as perceptual masking (PM) or adaptive steganography (AS) which can be applied in the spatial or frequency domain [1].

Here we present a wavelet steganographic scheme. The proposed method is capable of preventing visual degradation and providing a large embedding capacity. A wavelet domain preprocessing step is introduced before applying the proposed scheme to improve the steganography security [6, 7]. The embedding capacity for each pixel is determined by the local complexity of the cover image, allowing good visual quality as well as embedding a large amount of secret messages. These pixels are classified using a threshold based on the standard deviation of the local complexity of the cover image [7, 8]. Experimental results demonstrated that the proposed steganographic algorithm produces insignificant visual distortion due to the hidden message and provides high embedding capacity superior to that offered by the existing schemes. The proposed method is a secure steganographic algorithm due it can resist the image quality measures (IQM) steganalysis attack [4, 5, 8, 9]. Different colour spaces are incorporated in the proposed scheme (i.e. RGB, YCbCr and HSV) to ensure that the visual artifacts appeared in the stego-image are imperceptible and the differences between the cover and the stego-image are indistinguishable by the human visual system (HVS) [10, 11].

MATERIALS AND METHODS

Discrete Wavelet Transform and the Scaling Factor for Energy Adjustment: Wavelets provide a mathematical flexible tool for practical problems in science and engineering. One of the principal properties of the wavelets is that they allow modeling better processes that depend strongly on the time and whose behavior does

Corresponding Author: Dr. J. López-Bonilla, ESIME-Zacatenco, Instituto Politécnico Nacional, Col. Lindavista 07738, CDMX México.

not have for what to be smoothing. DWT is particularly effective for extracting information from non-periodical signals of finite life and it is closely linked to the analysis of multi-resolution (MRA), that is, see the signals at different frequencies [12], which allows to have a broader knowledge of the signal and facilitates the rapid calculation when the wavelet family is orthogonal [13-16].

It can be obtained wavelets $\left\{\psi_{j,n}(t)=\frac{1}{\sqrt{2^j}}\psi\left(\frac{t-2^j n}{2^j}\right)\right\}_{j,n\in Z^2}$ such that the family moved for *j* and dilated for *n,* it is a orthonormal basis of $L^2(IR)$. The orthogonal wavelets transport information about the changes of the signal to the resolution 2^{-j}. Then, the MRA appears: an image is modeled with orthogonal projections on vector space of different resolution, $P_{V_j}f, V_j \subset L^2(IR)$. The quantity of information in every projection depends on the size of V_j. For search orthogonal wavelets it will be necessary to work with approaches of multi-resolution [13-15, 17, 18]. For a function $f \in L^2(IR)$, the partial sum of the coefficients wavelet $\sum_{n=-\infty}^{\infty} < f, \psi_{j,n}$ can be interpreted as the difference between two approaches of *f* for the resolutions 2^{-1+j} and 2^{-j}. The multi-resolution approaches calculate the approach of signals to different resolutions with orthogonal projections in spaces $\{V_j\}_{j\in Z}$. The approach of a function of a resolution 2^{-j} is defined as an orthogonal projection in a space $V_j \in L^2(IR)$. The space V_j regroups all the possible approaches to the resolution 2^{-j}. The orthogonal projection of *f* is the function $f_j \in V_j$ that minimizes $\|f - f_j\|$. The orthonormal wavelets carry the necessary details to increase the resolution of the approach of the signal. The approaches of *f* for the scales 2^j and 2^{j-1} are respectively equal for its orthogonal projections V_j and V_{j-1} with $V_j \in V_{j-1}$. Be W_j the orthogonal complement of V_j in V_{j-1}. The orthogonal projection of *f* in V_{j-1} can be written as the sum of orthogonal projections *P* in V_j and W_j. Then, $P_{V_{j-1}}f = P_{V_j} + P_{W_j}$. The function $f(t) = A\sum_j\sum_n W_f(j,n)\psi_{j,n}(t)$ can be reconstructed from the discrete wavelets coefficients $W_j(j, n)$ where *j* is the scaling factor and *n* is the movement factor [13-15, 17, 18].

The wavelets $\psi_{j,n}(t)$ generated of the same wavelet mother function $\psi(t)$ have different scale *j* and place *n*, but they have the same form. Scale factor $j>0$ is always used. The wavelet is dilated when the scale $j>1$ and it is contracted when $j<1$. This way, changing the value of *j* the different range from frequencies is covered. Big values of the parameter *j* correspond to frequencies of minor range, or a big scale of $\psi_{j,n}(t)$. Small values of *j* correspond to frequencies of minor range or a very small scale of $\psi_{j,n}(t)$ [13-18]. The continuous wavelet functions with discrete factors of scale and movement are named discrete wavelets. Finally, the signal $f(t)$ can be compressed or expand in the time, this will have a few certain after effects in the plane of frequencies,

$$\begin{aligned} &f(t)\,compression\ by\ a\ factor\ 2^j\ (s)\, f_s(t) = \frac{1}{\sqrt{2^j}} f\left(\frac{t}{s}\right) \\ &\hat{f}(w)\,compression\ by\ a\ factor\ \frac{1}{2^j}\hat{f}_{2^j}(w) = \frac{1}{\sqrt{2^j}} 2^j \hat{f}\left(2^j w\right) = \sqrt{2^j}\,\hat{f}\left(2^j w\right) \end{aligned} \tag{1}$$

The coefficient of the decomposition of a function *f* in an orthogonal base of wavelets is calculated by a subsequent algorithm of discrete convolution with *h* and *g* and realizes a sampling of the low pass filter (LPF) $x_{low}[k] = \sum_n x[n]h[2k - n]$ and the high pass filter (HPF) $x_{high}[k] = \sum_n x[n]g[2k - n]$ where $g[2k-n]$ and $h[2k-n]$ are the impulse response of HPF and LPF, respectively, sub-sampled by a factor of 2 [17-20]. These coefficients are calculated by cascades of discrete filters through of convolution and sampling.

DWT decomposes a discrete signal into two sub-signals of half of the original length. This sub-signal is known as the approaches and the other one is known as the details [19]. The first sub-signal $a^1 = (a_1, a_2, \cdots, a_{m/2})$, for the signal *x* is obtained making the average of the signal as follows: The first value a_1 is calculated by taking the first set of values vector $x[m]: (x_1 + x_2)/2$ and multiplying it by $\sqrt{2}$, that is, $a_1 = (x_1 + x_2)/\sqrt{2}$, similarly $a_2 = (x_3 + x_4)/\sqrt{2}$, etc. In a general form, it is given by $a_{m/2} = x_{2m-1} + x_{2m}/\sqrt{2}$ where *m* is the vector size [19]. The other sub-signal is known as the first fluctuation of the signal *x* and it is denoted as: $d^1 = (d_1, d_2, \cdots, d_{m/2})$ and is calculated by taking the difference

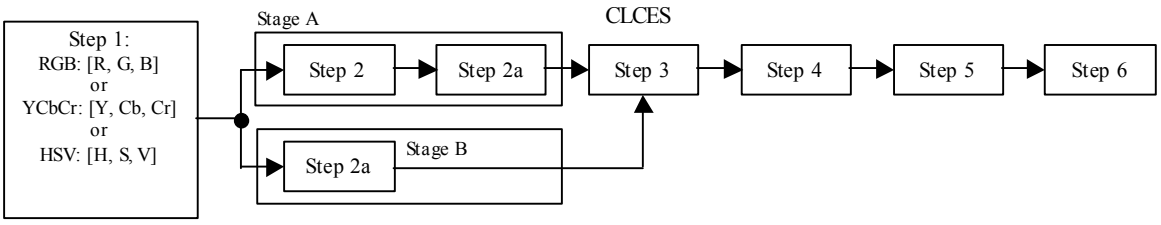

Fig. 1: Block diagram of the proposed CLCES method.

between the first pair of values of x, $(x_1–x_2)/2$ and then is multiplied and divided by $\sqrt{2}$ and so on. The final expression can be written as $d_{m/2} = x_{2m-1} - x_{2m}/\sqrt{2}$.

After applying the DWT are gotten two vectors, which are *approximations* and *details* obtained, with a length of half the original vector. Finally, continuing the recovery of the vector,

$$f[n] = \left\{\frac{a_1 + d_1}{\sqrt{2}}, \frac{a_1 - d_1}{\sqrt{2}}, \cdots, \frac{a_{n/2} + d_{n/2}}{\sqrt{2}}, \frac{a_{n/2} - d_{n/2}}{\sqrt{2}}\right\} \tag{2}$$

We note that the terms a_1 and d_1 in (6) and (7) can be interpreted as follows $\varepsilon_{\left(a^1 \middle| d^1\right)} = a_1 + \cdots + a_{n/2} + d_1 + \cdots + d_{n/2}$,

$$a_1 + d_1 = \left[\frac{f_1 + f_2}{\sqrt{2}}\right]^2 + \left[\frac{f_1 - f_2}{\sqrt{2}}\right]^2 = \frac{f_1^2 + 2f_1f_2 + f_2^2}{2} + \frac{f_1^2 - 2f_1f_2 + f_2^2}{2} = f_1^2 + f_2^2 \tag{3}$$

and similarly for each set of vectorial *approaches* and *details* [19]. So, the conservation of energy in wavelets is mentioned, the factor $1/\sqrt{2}$ is mentioned too [20, 21]. By applying the steganographic algorithm, it is necessary to use a scaling factor, but as the work is with an 8-bit RGB image, this scaling factor is closely related to energy conservation applied to wavelet theory for grayscale images as shown in most applications. However, for any space color we propose the following scaling factor [21],

$$1/\sqrt{2^j} \tag{4}$$

where j is directly dependent on the number of bits that integrate the image [20, 21].

The most common approach of the wavelet decomposition is to decompose an image to extract energy values for all sub-bands as features for the subsequent classification [21]. It is suitable to select a set of sub-bands for sparse representation in image classification applications. For a better classification of the results, it is desired that the energy features correspond to the areas of the selected sub-bands independent from each other as possible [21].

Proposed Steganographic Method: The proposed colour local complexity estimation based steganographic (CLCES) method is described in this section. The Figure 1 presents the block diagram of the steps used in the proposed method [8].

Step 1. Input the Cover Colour Image: We investigate the features of the RGB (Red, Green, Blue), HSV (Hue, Saturation, Value) and YCbCr (Luminance, Chromatic blue, Chromatic red) color spaces in the proposed algorithms to ensure that the visual artifacts appeared in the stego-images are imperceptible and the differences between the cover and the stego- images are indistinguishable by the HVS [10, 11]. Given a RGB cover colour image, the HSV and YCbCr transformations are computed [22]. Then, from each colour space we separate its colour components in an independent way and we apply in each component of the cover color image the next steps of the proposed methods.

Stage A: This stage improves the steganographic security and increases the embedding capacity by using the Step 2 [8]. The Step 2a is used to hide data.

Step 2. Cover Image Preprocessing: The preprocessing imposes more variation in pixel intensities of cover images compared to the original ones. It has been proved in [6] that the stego-images which carried out the hiding of secret data in the cover images with more variation in their pixel intensities are less detectable by the statistical

steganalysis increasing the embedding capacity [8]. Let propose a preprocessing step in the wavelet domain using the advantages of the wavelet decomposition [8]. The 1st-level Haar DWT and a redundancy of the approaches algorithm are used [7, 23-25]. The preprocessing step is applied in the sub-band LH of the cover image using a redundancy of the approaches algorithm. This algorithm is used because it is easy to implement, reduces the computational cost and provides good filtering results [7, 23-25]. The sub-band LH is chosen because it provides the information of the edges and the details of the cover image which are good locations to hide the data and besides with the preprocessing step there are more variations in the pixel intensities increasing the embedding capacity and improving the steganography security.

Step 2a. Apply 2nd-level Daubechies db4 DWT: This step is used to hide data. Let use the sub-band LH obtained from the wavelet coefficients of the sub-band LL from the 2nd decomposition of the resulting image of the step 2. The decomposition level and the Daubechies db4 are selected according with the extensive experimental results realized with different wavelet families under objective criteria [8, 26-29].

Stage B: This stage allows having more hiding capacity in the proposed method because it provides more decomposition levels to hide information [8].

Step 2a. Apply 2nd-level Daubechies db4 DWT. This step is the same discussed above.

The next steps are applied in both outputs of the stages A and B providing more hiding capacity [8].

Step 3. Standard Deviation Computation: The embedding capacity for each pixel is determined by the local complexity of the cover colour image providing a good visual quality as well as embedding a large amount of secret messages [6]. From the wavelet decomposition let use the standard deviation $\sigma_k = \sqrt{\sum_{m=1}^{n}(x_m - \bar{x})^2 / n}$ of the sub-band LH obtained from the wavelet coefficients from the sub-band LL of the 2nd decomposition of the cover colour image using a 3x3 kernel, where x_m is an element of the current kernel k, $\bar{x} = \sum_{m=1}^{n} x_m / n$ is the mean value of current kernel and $n = 9$ is the number of elements in the sample [8, 27, 30].

Step 4. Threshold Computation: The pixels are classified using a threshold based on the local complexity of the standard deviation in the cover image. The threshold $T = \sum_s \left(\alpha_s \cdot 2^{-s}\right) \Big/ \sum_s 2^{-s}$ is used to select the pixels whose values are considered as places to hide data [31, 32], where T denotes a threshold value for discriminating signal-dominant scales from the noise dominant ones, s is the level or scale used in the wavelet analysis (s=1 and s=2 for Haar and db4 wavelets, respectively), $\alpha_s = \sigma_k$ is the standard deviation of the current wavelet coefficient kernel in the s level and 2^{-s} is the weighting function [8, 25, 31].

Step 5. Robust Criterion to Hide Data: The image quality of the processed images is improved using a criterion based on the median estimator. The condition $\beta_{sx} \geq T$ is applied for each kernel of the standard deviation $\alpha_s = \sigma_k$, if this condition is satisfied then this area or region is considered noisy and thus can be inserted the information to hide in the respective wavelet kernel coefficients H_k of the cover colour image [8],

$$S_k = \begin{cases} D_k, & \beta_{sx} \geq T \\ H_k, & \text{otherwise} \end{cases} \quad (5)$$

where $\beta_{s1} = |\ \sigma_c - \text{MED}(\alpha_s)|$ and $\beta_{s2} = \text{MED}(\alpha_s)$ are the two robust criteria to hide data [26, 27], MED(α_s) is the median of the wavelet kernel coefficients α_s and σ_c is the standard deviation located in the center of the kernel α_s. We propose the use of median as a robust estimation of the energy [21, 32] of the wavelet kernel coefficients given by its local standard deviation. These procedures improve the features of the proposed method to provide good invisibility, color retention and fine detail preservation of the processed images [8].

To recover the hidden image, the algorithm is used again but in the step 1 the input changes from the cover color image to the stego-image and to repeat the same steps changing the conditions of the step 5 to recover the hidden data in the following way [8],

$$D_k = \begin{cases} S_k & \alpha_s < T \\ H_k & \text{otherwise} \end{cases} \quad (6)$$

$$D_k = \begin{cases} S_k, & \beta_{sx} \geq T \\ H_k, & \text{otherwise} \end{cases} \quad (7)$$

Other versions of the CLCES algorithm are given by using a threshold based on the median of the

standard deviations in the current wavelet kernel coefficient in the level s changing the threshold of $T = \sum_s \left(\alpha_s \cdot 2^{-s}\right) \Big/ \sum_s 2^{-s}$ to $T_i = \text{MED}\{\alpha_s\}$ [8].

Step 6. Inverse Discrete Wavelet Transform (IDWT) Computation: We obtain the resulted stego-image applying the IDWT to the wavelet coefficients of the stego-image (Figure 1).

DISCUSSION

The purpose of this research is to propose a simple steganographic algorithm implementation, with little resource consumption on mobile devices, where the results were qualitative, quantitative and highly acceptable steganalysis. The purpose of steganography is to insert hidden information on a digital file, thus achieving high resource utilization. We present the results better PSNR, MAE, CC and Q for a scaling factor when j = 9. Through analysis of steganalysis is determined the probability of detection of hidden information exceeds 95%, higher than the results reported in classical literature.

RESULTS

The proposed CLCES method is evaluated [8] and its performance is compared with the LSB (Least Significant Bit) [33] steganographic method. We also adapt the LSB method [33] to work in the wavelet domain using the 2nd-level Daubechies db4 DWT to compare our proposal, in here this method is named as WLSB. The image quality of various schemes is compared in terms of the PSNR (Peak Signal-to-Noise Ratio), the MAE (Mean Absolute Error), the NCD (Normalized Color Difference), the CC (Cross-Correlation), the Q (Quality index) and the HC (Hiding Capacity) criteria [1, 4, 5, 7, 25, 33-35].

In our experiments we use the 320x320 color images 'Lena' and 'Mandrill' and we present the results of several steganographic methods for the RGB, HSV and YCbCr colour spaces. The performance results for the stego-image "Mandrill" (the secret image "Lena") and the retrieved secret image "Lena" are shown in the Tables 1 and 2, respectively.

From the experimental results from the Table 1 and Table 2 we depict in the Figure 2 the subjective visual results (zoom parts) using the RGB colour space. We observe from the error stego-images that the

Table 1: Performance results for the stego-image 'Mandrill' with the secret image 'Lena'

	Criteria for the RGB colour space					
Algorithms	PSNR dB	MAE	CC	Q	NCD	HC (Kb)
LSB	34.5602	3.5758	0.9978	0.9977	7.3506e-4	1.9199e3
WLSB	28.8347	8.8469	0.9977	0.9963	0.0053	0.8352e3
CLCES (β_{s1})	38.2650	1.4503	0.9983	0.9984	2.5473e-4	1.9183e3
CLCES (β_{s2})	38.5287	1.4417	0.9984	0.9985	2.3584e-4	1.8698e3
CLCES (T_1,β_{s1})	38.9540	1.3910	0.9985	0.9986	2.3017e-4	1.7980e3
CLCES (T_1,β_{s2})	38.4697	1.4478	0.9984	0.9984	2.4352e-4	1.8804e3
			Criteria for the YCbCr colour space			
LSB	28.0065	7.1783	0.9889	0.9886	0.0081	1.9859e3
WLSB	26.0195	7.3820	0.9885	0.9883	0.0086	0.8277e3
CLCES (β_{s1})	28.2348	4.3867	0.9857	0.9866	9.5800e-4	7.1724e3
CLCES (β_{s2})	28.5554	4.4563	0.9870	0.9878	0.0013	6.7308e3
CLCES (T_1,β_{s1})	28.2612	4.4212	0.9858	0.9867	0.0013	7.1355e3
CLCES (T_1,β_{s2})	28.1469	4.3067	0.9853	0.9862	0.0012	7.2982e3
			Criteria for the HSV colour space			
LSB	26.0193	4.2270	0.9795	0.9801	0.0071	1.1578
WLSB	26.0155	4.2287	0.9795	0.9801	0.0073	0.7553
CLCES (β_{s1})	26.5489	4.1678	0.9831	0.9830	0.0072	5.2464
CLCES (β_{s2})	25.8352	4.4367	0.9803	0.9803	0.0079	5.0933
CLCES (T_1,β_{s1})	26.6850	4.1304	0.9833	0.9833	0.0071	5.1190
CLCES (T_1,β_{s2})	26.0651	4.2298	0.9810	0.9815	0.0077	5.2505

Table 2: Performance results for the retrieved secret image 'Lena'

	Criteria for the RGB colour space				
Algorithms	PSNR dB	MAE	CC	Q	NCD
LSB	36.1233	2.7714	0.9955	0.9962	0.00200
WLSB	31.2219	5.0316	0.9954	0.9954	0.00330
CLCES (β_{s1})	36.1233	2.7714	0.9955	0.9962	0.00200
CLCES (β_{s2})	36.1233	2.7714	0.9955	0.9962	0.00200
CLCES (T_1,β_{s1})	36.1233	2.7714	0.9955	0.9962	0.00200
CLCES (T_1,β_{s2})	36.1233	2.7714	0.9955	0.9962	0.00200
			Criteria for the YCbCr colour space		
SB	36.0827	2.7948	0.9954	0.9962	0.00200
WLSB	36.0821	2.7948	0.9954	0.9962	0.00200
CLCES (β_{s1})	36.0827	2.7948	0.9954	0.9962	0.00200
CLCES (β_{s2})	36.0827	2.7948	0.9954	0.9962	0.00201
CLCES (T_1,β_{s1})	36.0827	2.7948	0.9954	0.9962	0.00200
CLCES (T_1,β_{s2})	36.0827	2.7948	0.9954	0.9962	0.00200
			Criteria for the HSV colour space		
LSB	36.1222	2.7740	0.9954	0.9962	0.00200
WLSB	36.1222	2.7790	0.9954	0.9962	0.00200
CLCES (β_{s1})	36.1201	2.7730	0.9951	0.9959	7.8233e-4
CLCES (β_{s2})	36.1201	2.7730	0.9951	0.9959	7.8233e-4
CLCES (T_1,β_{s1})	36.1201	2.7730	0.9951	0.9959	7.8233e-4
CLCES (T_1,β_{s2})	36.1201	2.7730	0.9951	0.9959	7.8233e-4

Fig. 2: Subjective visual results for the stego-image 'Mandrill' with the secret image 'Lena' showing the stego-image, the error stego-image, the retrieved secret image and the retrieved error secret image from the left to the right for each method. Row 1: a)-d) using LSB, Row 2: e)-h) CLCES(T_1,β_{s1})

proposed method provides less distortion in comparison with the LSB method. In the case of retrieved secret error images the proposed methods provide similar subjective visual results and in some cases (see the NCD of the Table 2) the proposed method outperforms the comparative methods. We can see that the images produced with the proposed CLCES methods appear to have a very good subjective quality [8].

Applying the proposed scaling scheme can be seen an improvement in visual images [21]. In the case of different j values in the scaling factor by using the same images "Mandrill" [12] as cover image and "Lena" [12] as hide image, in Table 3, one can see when the j value increases the performance results increase too.

Figure 3 depicts the processed images for stego-image "Mandrill" (Figure 3a-b-c) and retrieved secret image "Lena" (Figure 3d-e-f) according with Table 3. We observe from Figure 3 c) and f) that the best results are obtained when j = 9, where j represents the number of bits resolution of the image to hide. It is observed that when j is gradually increase the quality image is significantly improved. From Figure 3d, 3e and 3f one can see that

Table 3: Performance results for different values of *j* with cover image "Mandrill" and hidden image "Lena".

Proposed method		PSNR db	CC	NCD	Q	MAE
j=0	Cover image	31.5084	78.52	--------	0.7836	10.4878
	Recovered image	16.5327	38.80	0.4748	0.3586	4.9403
j=2	Cover image	31.4999	80.46	--------	0.8040	9.9490
	Recovered image	16.9537	38.89	0.4749	0.3587	4.9471
j=5	Cover image	36.1233	97.81	0.0020	0.9792	3.2086
	Recovered image	27.2474	99.85	0.0020	0.9962	2.7714
j=9	Cover image	36.1233	99.08	8.015e-4	0.9913	2.0309
	Recovered image	31.0781	99.80	0.0020	0.9962	2.7714
j =10	Cover image	36.1233	99.34	6.0486e-4	0.9934	1.7022
	Recovered image	32.5167	99.55	0.0020	0.9962	2.7714

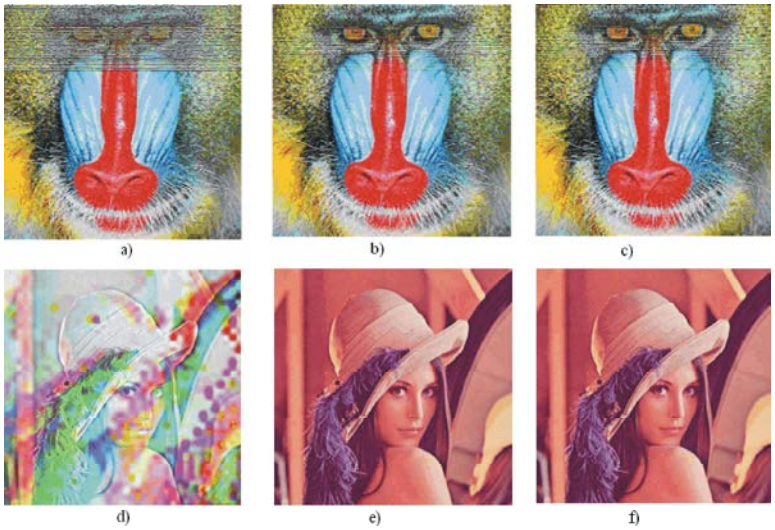

Fig. 3: Visual results for different values of j in the scaling factor, a) and d) column with =2, b) and e) column with =5, and c) and f) =9.

when the value of proposed scaling factor increases the subjective quality of images increases too, it is observed that Figures 3a), b) and c) have in the upper part a certain lineal distortion, which can be interpreted as external information inserted to the cover image. As j takes the value of 10 or 24 of this lineal distortion in the top of the stego-image not easily identified visually. We also present the wrong images.

More tests were performed to increase the value of *j* to *j* = 24, amount determined by the image type here manipulated. It was observed those significant changes of stego-image and the recovered image. Figure 4 presents the visual results for *j*=10. The proposed scaling factor $1/\sqrt{2^j}$ for each test presents a different result as can be seen in the previous tests, the scaling factor does not affect the steganographic algorithm and preserving the energy of images [21]. It can be seen in the Lena error image of Figure 4d, the difference in values between the host image and the recovered image is approximately zero.

The results shown in Table 4 using the scaling factor *j* = 24, we can that these are superior to those shown in Table 4. Being the best method LSB with PSNR equal to 34.5602 dB thing which is exceeded by the second PSNR of 36.7973 dB with *j* = 24 [21].

We realize experiments of steganalysis attack to measure the robustness capabilities of several steganographic algorithms using the well-known Image Quality Measures (IQM) steganalysis [4, 5, 8, 9]. The IQM steganalysis technique provides good results across all steganographic algorithms (i.e. spread-spectrum, quantization modulation, LSB, etc.) [4, 5, 8, 9]. In this technique has been observed that filtering an image without embedded data causes changes in the IQMs less than the changes brought about on embedded images [8,13]. The IQMs used to compare different methods are: the MSE (Mean Square Error), the Czekanowski Distance (CD), the Angular Correlation (AC), the Image Fidelity (IF), the Normalized Cross-Correlation (NCC), the Spectral Magnitude Distortion (SMD), the Median of Block

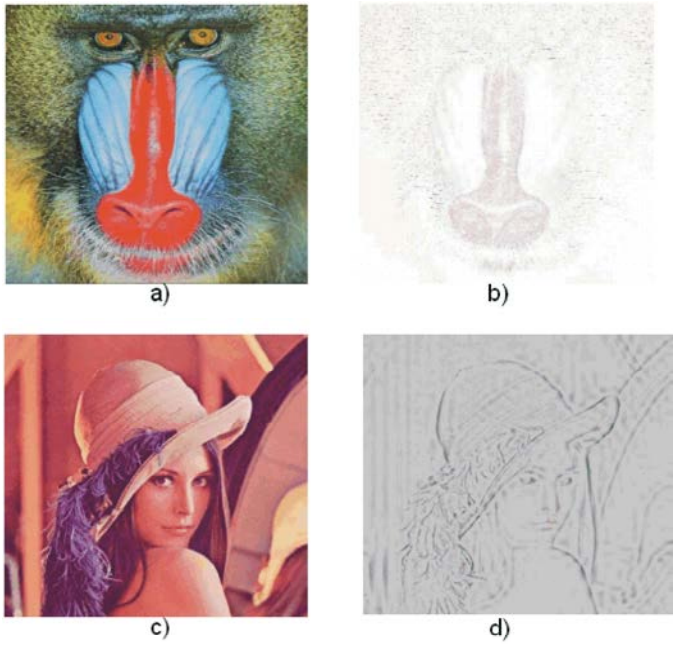

Fig. 4: Visual results in the case of j = 10, a) host image "Mandrill, b) error image "Mandrill, c) hide image "Lena", d) error image "Lena".

Table 4: Performance results in the case of j = 24 in the scaling factor with cover image "Mandrill" and hidden image "Lena"

Cover image "Mandrill"	Hide image "Lena"
Q=0.9968	Q=0.9962
PSNR=36.7973 dB	PSNR=36.1232 dB
CC=99.67%	CC=99.56%
NCD=5.7204 e-4	NCD=19.735e-4
MAE=1.4721	MAE=2.7714

Table 5: Total detection of the hidden data using the image quality measures (IQM) steganalysis

	Stego-image 'Mandrill' (secret image 'Lena')		
Algorithms	RGB	YCbCr	HSV
LSB	4/9	2/9	4/9
WLSB	4/9	3/9	5/9
CLCES (β_{s1})	3/9	3/9	2/9
CLCES (β_{s2})	3/9	3/9	2/9
CLCES (T_1,β_{s1})	3/9	2/9	2/9
CLCES (T_1,β_{s2})	3/9	2/9	2/9

Spectral Phase (MBSP), the Median of Weighted Block Spectral Distortion (MWBSD) and the Normalized Mean Square HVS Error (NMSHVSE) [4, 8, 9]. We obtain the performance of different steganographic algorithms, using the condition IQMcover = IQMstego means that the image contains the hidden data, otherwise, it does not [8].

The Table 5 shows the total detection of the hidden data using the results of IQMs steganalysis for the cover image 'Mandrill' and its filtered version and the stego-image 'Mandrill' with the secret image 'Lena' and its filtered version [8]. Comparing the steganalysis results with the image quality of the stego-images and the hiding capacity of the methods, we comment that the proposed CLCES methods [8] outperform other methods by balancing the image quality and the embedding capacity providing a better security against attacks of steganalyzers in comparison with the other methods [8].

CONCLUSIONS

By applying the proposed scaling factor $1/\sqrt{2^j}$ in a color image, there is an adjustment factor for the energy input in each sub-matrix. It is also noted that when is changing the value of j, it adjusts the sharpness and image clarity providing a visible improvement of the visual image.

The CLCES method uses thresholds based on the standard deviation of the local complexity of the cover image to provide a compromise between the embedding capacity and the image visual quality. Different colour spaces are incorporated in the proposed schemes to ensure that the differences between the cover and stego-images are indistinguishable by the HVS. The proposed CLCES method is a secure steganographic method outperforming other methods by balancing the image quality and the embedding capacity providing a better security against attacks of steganalyzers in comparison with other methods. Finally, the proposed scheme is simple, efficient and feasible for the adaptive steganographic applications.

REFERENCES

1. Cheddad, A., J. Condell, K. Curran and P. Mc Kevitt, 2010. Digital image steganography: Survey and analysis of current methods. Signal Processing, 90: 727-752.
2. Petitcolas, F.A.P., R.J. Anderson and M.G. Kuhn, 1999. Information hiding – a survey. Proc. IEEE, 87(7): 1062-1078.
3. Petticolas, F. and S. Katzenbeisser, 2000. Information *Hiding Techniques for Steganography and* Digital Watermarking, Artech House: Boston, (2000).
4. Luo, X.Y., D.S. Wang, P. Wang and F.L. Liu, 2008. A review on blind detection for image steganography. Signal Processing, 88: 2138-2157.
5. Kharrazi, M., H.T. Sencar and N. Memon, 2006. Performance study of common image steganography and steganalysis techniques. Journal of Electronic Imaging, 15(4): 1-16
6. Sajedi, H. and M. Jamzad, 2010. BSS: Boosted steganography scheme with cover image preprocessing. Expert Systems with Applications, 37: 7703-7710.
7. Gallegos-Funes, F.J., J. Martínez-Valdés and J.M. De-la-Rosa-Vázquez, 2007. Order Statistics Filters in Wavelet Domain for Color Image Processing. IEEE Sixth Mexican Int. Conf. on Artificial Intelligence, MICAI2007, pp: 121-130.
8. Carvajal-Gámez, B.E., F.J. Gallegos-Funes and A.J. Rosales-Silva, 2013. Color local complexity estimation based steganographic (CLCES) method. Expert Systems with Applications 40: 1132-1142.
9. Avcibas, I., N. Mmon and B. Sankur, 2003. Steganalysis using image quality metrics, IEEE Trans. Image Process., 12(2): 221-229.
10. Cheddad, A., J. Condell, K. Curran and P. Mc Kevitt, 2008. Biometric Inspired Digital Image Steganography. 15th IEEE Int. Conf. and Workshop on the Engineering of Computer Based Systems, ECBS2008, Belfast, Northern Ireland, pp: 159-168.
11. Liu, K.C., 2010. Wavelet-based watermarking for color images through visual masking. Int. J. Electron. Commun. (AEÜ), 64: 112-124.
12. Vetterli, M. and J. Kočević, 1995. Wavelets and sub-*band coding*, Ed. 2th; Prentice-Hall: New Jersey, (1995).
13. Petrosian, A. and F. Meyers, 2002. Wavelets in signal and image analysis. Computational imaging and vision, Springer: Berlin, (2002).
14. Debnath, L., 2002. Wavelets and Signal Processing, Birkhauser: Berlin, (2002).
15. Sheng, Y., 2002. The transforms and applications handbook, Ed. 2th; CRC Press: London, (2002).
16. Bogges, A. and F. Narcovich, 2009. A first course in wavelets with Fourier Analysis, 2th Ed., Wiley: New York, (2009).
17. Daubechies, I., 1988. Orthonormal bases of compactly supported wavelets. Communications on Pure Applied Mathemathics, 41: 909-996.
18. Mallat, S., 1989. A theory for multiresolution signal decomposition: the wavelet representation. IEEE Transactions on Pattern Analysis and Machine Intelligence, 11(7): 674-694.
19. Walker, J., 2003. A primer on wavelets and their scientific applications, Ed. 2th; Chapman and Hall/CRC: London, (2003).
20. Carvajal-Gámez, B.E., F.J. Gallegos-Funes and J. López-Bonilla, 2010. Computational Techniques and algorithms for Image Processing. Ed. Lambert Academic Pub: Berlin, Chap., pp: 13.
21. Carvajal-Gámez, B., F.J. Gallegos-Funes, A.J. Rosales-Silva and J. López-Bonilla, 2013. Adjust of energy with compactly supported orthogonal wavelet for steganographic algorithms using the scaling function, International J. Phys. Sci., 8(4): 157-166.
22. Alata, O. and L. Quintard, 2009. Is there a best color space for colour image characterization or representation based on Multivariate Gaussian Mixture Model? Computer Vision and Image Understanding, 113: 867-877.
23. De Queiroz, R.L., 2010. Reversible color-to-gray mapping using sub-band domain texturization. Pattern Recognition Letters, 31: 269-276.
24. Ashwin, A.C., K.R. Ramakrishnan and S.H. Srinivasan, 2003. Wavelet domain residual redundancy based descriptions. Signal Processing: Image Commun, 18: 549-560.
25. Gallegos-Funes, F.J., B.E. Carvajal-Gámez, J. López-Bonilla and V.I. Ponomaryov, 2010. Steganographic method based on wavelets and center weighted median filter, IEEE Int. Kharkov Symposium on Physics and Engineering of Microwaves, Millimeter and Submillimeter Waves, MSMW2010, Kharkov: Ukraine (2010).
26. Maheswaran, R. and R. Khosa, 2012. Comparative study of different wavelets for hydrologic forecasting. Computers and Geosciences, doi.org/10.1016/j.cageo.2011.12.015 (2012).

27. Huang, K. and S. Aviyente, 2006. Information-theoretic wavelet packet sub-band selection for texture classification. Signal Processing, 86: 1410-1420.
28. Lo, S.C.B., H. Li and M.T. Freedman, 2003. Optimization of Wavelet Decomposition for Image Compression and Feature Preservation. IEEE Trans. Medical Imaging, 22(9): 1141-1151.
29. Nafornita, C. and A. Isar, 2009. On the Choice of the Mother Wavelet for Perceptual Data Hiding. Int. Symp. Signals, Circuits and Systems, ISSCS 2009, pp: 1-4.
30. Cheddad, A., J. Condell, K. Curran and P. Mc Kevitt, 2008. Biometric Inspired Digital Image Steganography. 15th IEEE Int. Conf. and Workshop on the Engineering of Computer Based Systems, ECBS2008, pp: 159-168.
31. Gallegos-Funes, F.J., J. Martinez-Valdes and J.M. De-la-Rosa-Vazquez, 2007. Order Statistics Filters in Wavelet Domain for Colour Image Processing. IEEE Sixth Mexican Int. Conf. on Artificial Intelligence, MICAI2007, pp: 121-130.
32. Carvajal-Gámez, B.E., F.J. Gallegos-Funes and J. López-Bonilla, Energy adjustment RGB images in steganography applications. 52nd IEEE Int. Midwest Symp. Circuits and Systems, Cancun: Mexico, pp: 758-761.
33. Chan, C.K. and L.M. Cheng, 2004. Hiding data in images by simple LSB substitution. Pattern Recognition, 37: 469-474.
34. Gallegos-Funes, F.J., A J. Rosales-Silva and A. Toledo-López, 2012. Multichannel image processing by using the Rank M-type L-filter. Journal of Visual Communication and Image Representation 23(2): 323-330.
35. Yu, Y.H.; C.C. Chang and I.C. Lin, 2007. A new steganographic method for colour and Grayscale image hiding. Computer Vision and Image Understanding, 107: 183-194.